

A nickel molybdenite cathode for the hydrogen evolution reaction in alkaline media

L. B. ALBERTINI, A. C. D. ANGELO*, E. R. GONZALEZ

Instituto de Física e Química de São Carlos/USP, C.P. 369, 13560, São Carlos, SP, Brazil

Received 2 August 1991; accepted 5 February 1992

The characteristics and mechanism of the hydrogen evolution reaction on a nickel sulphide electrode incorporating molybdenite particles are described. At 25°C the overpotential for the reaction is 300 mV lower than that of the mild steel cathodes used in unipolar electrolyzers. The material shows good stability under long term operation.

1. Introduction

The possibility of using hydrogen as a clean fuel together with an increasing concern for the depletion of fossil fuels and environmental problems have been strong incentives for R&D activities on electrolytic hydrogen. Today, the cost of hydrogen production by this means is higher than that obtained from fossil fuels and so efforts are being directed toward the reduction of production costs. Cost depends on several factors, the result of which is directly proportional to the operational voltage of the electrolyser. Because of this, there is an interest in finding better electrode materials with electrocatalytic activity.

Several electrode materials, mainly based on the modification of nickel surfaces by codeposition of other elements, have been found to have electrocatalytic activity toward the hydrogen evolution reaction (HER) in alkaline media [1–8]. In particular, compounds containing sulphur have shown promising characteristics under those conditions [4–8].

Vandenborre *et al.* [5] studied nickel sulphide cathodes obtained from a nickel electrodeposition bath using thiourea as a source of sulphur. Based on the analysis of Tafel plots the authors proposed that the HER follows a Volmer–Heyrovsky mechanism. The electrode showed enhancement of its activity after a few hours of polarization which was interpreted as being a consequence of the increasing amount of hydrogen dissolved in the cathode.

Nidola and Schira [7] examined a series of electrode materials based on transition-metal sulphides. In general they observed a gradual deactivation during electrolysis, which was attributed to the plating of iron impurities on the cathodes.

Sabela and Paseka [8] also reported results on NiS. Under polarization, an initial decrease in overpotential was observed and was attributed to a ‘cleaning’ process that leached out some of the sulphur at the surface, leaving a highly active structure. After a few hours, however, the overpotential increased. Accord-

ing to the authors this was due to the deposition of iron impurities.

One interesting aspect of the NiS_x material is the report of Nidola and Schira [7] that the addition of MoS₂ as a pigment in the electrodeposition bath produces an electrodeposit that maintains its activity for periods of up to 2000 h and suffers no deleterious influence of the iron impurities. This was interpreted as due to the stabilization of the NiS_x matrix by MoS₂ particles.

In view of these findings it was considered worthwhile to carry out more detailed studies on this material in order to better understand the participation of the MoS₂. Also, taking in account possible practical applications, the use of natural molybdenite instead of reagent grade MoS₂ was examined. Preliminary tests of a NiS_x–MoS₂ cathode were also performed under the working conditions of a chlor-alkali cell.

2. Experimental details

Electrodes were prepared by mounting mild steel substrates (0.006% C, 0.06% P, 0.55% Mn and 0.022% S) into epoxy resin [1], leaving an exposed geometric area of 0.5 cm². Prior to electrodeposition the surface was treated with emery paper and cleaned with dilute HCl and acetone. Nickel was deposited first, using a modified Watts bath. The codeposition of molybdenite particles was done on this surface using a second bath. The composition of the baths and the electrodeposition conditions are given in Table 1. All the reagents used were p.a. quality. The natural molybdenite was produced in Rio Grande do Norte, Brazil. The mineral was ground and used as particles of 20–30 µm. No foreign materials were detected when X-ray diffractograms of this product were compared with reagent grade MoS₂.

Three different electrodes were prepared and studied comparatively. These were:

E1 = an electrode with electrodeposited nickel on mild steel;

* Present Address: Departamento de Química, UNESP, Bauru, C.P. 473, Bauru, São Paulo, 17100, Brazil. Author to whom correspondence should be addressed.

Table 1. Composition of the baths and electrodeposition conditions for the preparation of the cathodic materials

Bath	$\text{NiSO}_4/$ g dm^{-3}	$\text{NiCl}_2/$ g dm^{-3}	$\text{H}_3\text{BO}_3/$ g dm^{-3}	$\text{Na}_2\text{S}_2\text{O}_3/$ g dm^{-3}	Molybdenite/ g dm^{-3}	pH	$T/^\circ\text{C}$	$i/\text{mA cm}^{-2}$	t/min
Nickel	300	45	30	—	—	4.5	60	20–80	30
Pigmentation	120	25	—	2	0.02	2.5	30	25	30

T : Temperature, i : current density and t : deposition time.

E2 = the same as E1 but subjected to electrodeposition in the pigmentation bath without molybdenite.

E3 = the same as E2 with molybdenite present in the pigmentation bath.

The average thickness of the deposits was of the order of $40\text{ }\mu\text{m}$. The morphology and the qualitative composition of the electrode surfaces were determined with a Cambridge Stereoscan scanning electron microscope. Electrochemical experiments consisted of steady-state polarization curves and cyclic voltammetry. These were carried out using a PAR Mod 273 Potentiostat and a three compartment glass cell. Most measurements were carried out without taking into account the uncompensated solution resistance because, in the low current density region, currents were essentially similar to those corrected by using the current interruption technique. A platinum sheet (2 cm^2) served as auxiliary electrode and a $\text{Hg}[\text{HgO}]\text{HO}^-$ (28%), joined to the main compartment through a Luggin capillary, as reference electrode. At 25°C the equilibrium potential for hydrogen in this scale is -0.932 V .

KOH (Merck p.a.) and NaOH (Merck p.a.) + NaCl (Merck p.a.) solutions were pre-electrolysed for 120 h at 1 A cm^{-2} under stirring using platinum electrodes in order to eliminate iron impurities. The ratio of the electrode surface to the solution volume was 0.013 cm^{-1} . The iron impurities were collected as a black deposit on the cathode. No platinum was detected in the solution after this treatment. Polarization curves as a function of pH were obtained in NaOH (Merck p.a.) + NaClO_4 (Merck p.a.) sol-

utions maintained at an ionic strength of 6.29 M in order to minimize double layer effects. This ionic strength is the same as that of a 28% KOH solution.

3. Results and discussion

Figure 1 shows Tafel plots for the HER on the electrodes E1, E2 and E3. The corresponding Tafel parameters are presented in Table 2, together with those for the conventional material (mild steel) used in unipolar electrolyzers. Two plots are presented in Fig. 1 for electrodes containing MoS_2 : one using molybdenite and the other using reagent grade MoS_2 . The results show that there is essentially no difference between the two materials.

From Fig. 1 it can be concluded that in the second electrodeposition process the enhanced performance of the electrode appears more pronounced, particularly at high current densities, when the molybdenite particles are incorporated into the surface. In principle this may be due to an increase in active surface area or to a true electrocatalytic effect or both. This aspect was analysed with the help of the results of the morphological and surface characteristics studies.

Figure 2 shows SEM micrographs of the electrodes E1, E2 and E3. It is apparent that the second deposition produces a substantial increase in active surface area. However, the incorporation of molybdenite particles does not alter the morphology of the surface. This is also confirmed by voltammetric studies. Figure 3 presents voltammograms of electrodes E1, E2 and E3, respectively. In this study it was observed that the anodic process corresponds to the reaction:

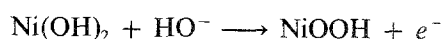


Table 3 presents the charges corresponding to this anodic process which confirms a marked increase in the effective surface area of the electrode E2 with respect to E1. However, the electrochemically active surface areas of the electrodes E2 and E3 are very similar, indicating that molybdenite particles have no

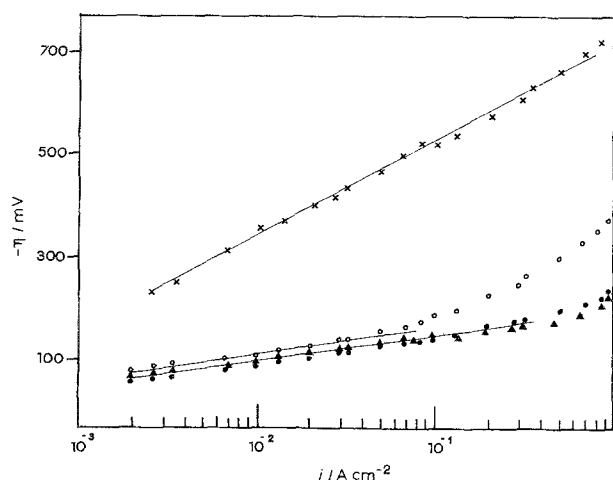


Fig. 1. Tafel plots for the HER on the different electrodes in 28% KOH and 25°C . (x) E1, (o) E2, (●) E3 and (▲) E3 using molybdenum sulphide.

Table 2. Electrochemical parameters of the HER on the different electrode materials in 28% KOH at 25°C

Electrode	$b/\text{mV dec}^{-1}$	$-\eta_{135}/\text{mV}$	$i_0 \text{ ap.}/\text{A cm}^{-2} \times 10^4$
E1	184	579	1.29
E2	64	188	3.64
E3	52	138	1.80
Mild steel	192	447	3.64

b : Tafel slope in the low c.d. region, i_0 : exchange current, η_{135} : overpotential at c.d. 135 mA cm^{-2} .

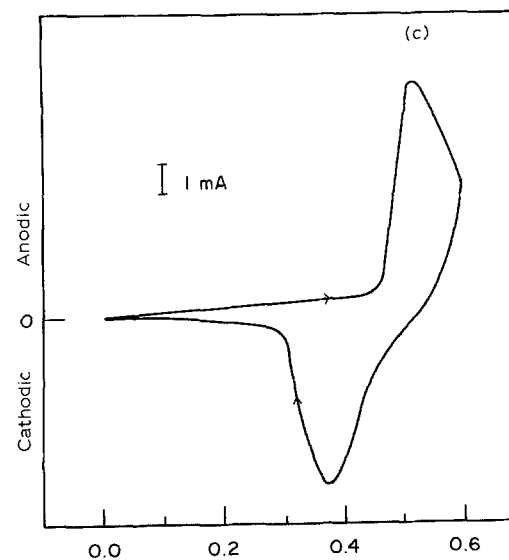
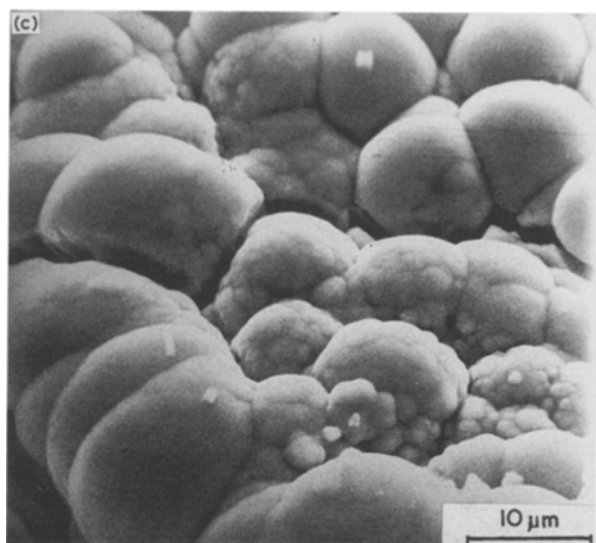
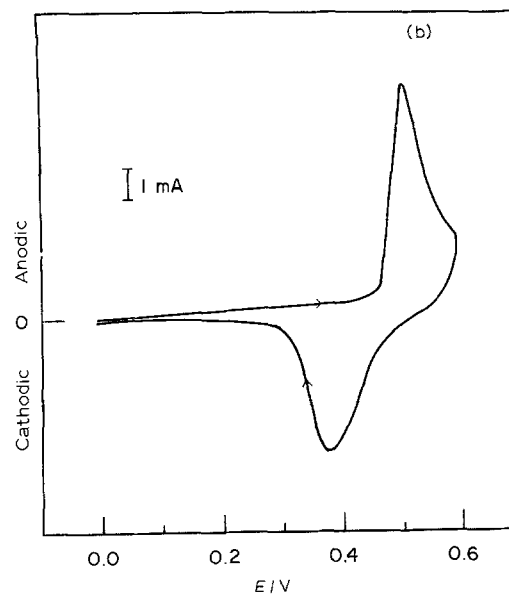
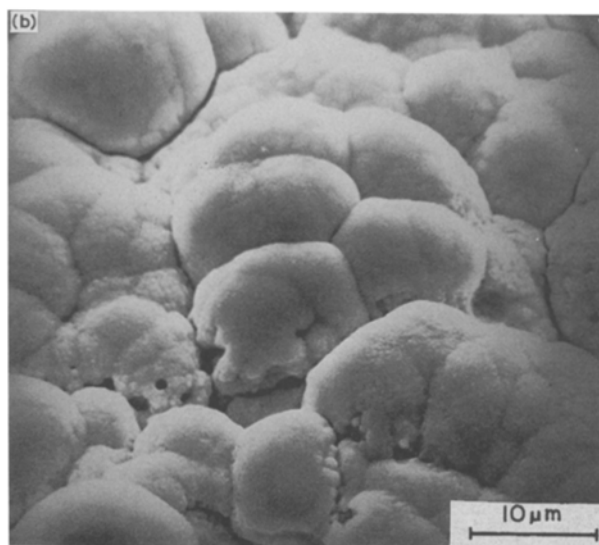
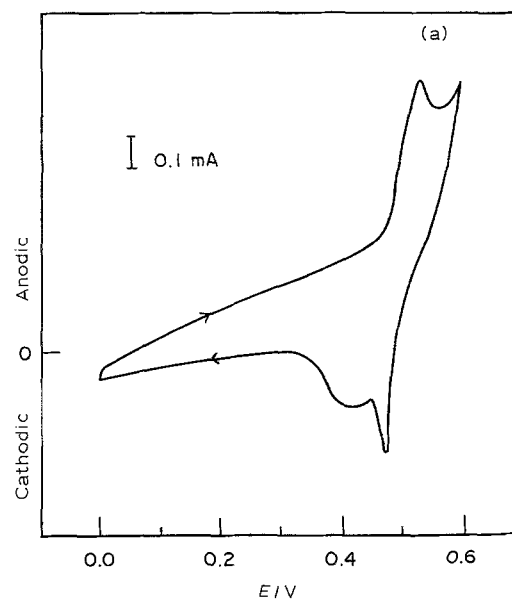
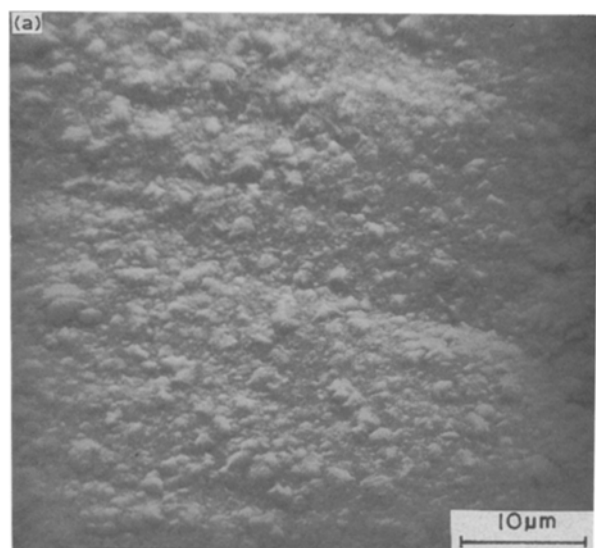


Fig. 2. SEM micrographs of the electrodes: (a) E1, (b) E2 and (c) E3.

Fig. 3. Cyclic voltammograms for the electrodes (a) E1, (b) E2 and (c) E3 in 1 N KOH solution at 25°C. $v = 50 \text{ mV s}^{-1}$.

Table 3. Electrochemical anodic charges (Q_a) for the electrodes E1, E2 and E3, calculated from the voltammograms in Fig. 3

Electrode	Q_a/mc	Roughness factor*
E1	0.82	1
E2	10.03	12
E3	12.10	14

* With respect to the electrode E1.

influence on this parameter. Thus, it must be concluded that the better performance of the electrode containing molybdenite is due, not only to an increase in the surface area, but to an enhanced catalytic effect.

This may be explained on the basis of the electrode structure of the elements forming the alloy. A synergistic effect in the hydrogen evolution reaction has been observed on binary alloys of transition metals, one of them having vacant semi-d-orbitals and the other available paired d-electrons [12]. This is because the hydrogen ion requires an electron pair to adsorb, while the hydrogen adatom requires an empty d-orbital. The enhanced catalytic effect of these hypo-hyper-d-electronic combinations of transition metals may be extended to their compounds. Thus Chianelli *et al.* [13] found a synergistic effect in hydrodesulphurization reaction on mixtures of sulphides, like Co-Mo and Ni-Mo dichalcogenide couples. A volcano curve with the maximum around nickel is found in the 3d transition metals row which points to a similarity in the characteristics of electrocatalysis between the hydrogen evolution and the hydrodesulphurization reactions.

In order to evaluate the effect of temperature on the electrode E3, Tafel plots were obtained in 28% KOH in the range 25–80°C. These are shown in Fig. 4 and the corresponding Tafel parameters are given in Table 4. At low current densities no significant change in Tafel slope is observed. This is unexpected because classical electrochemical theory based in the Butler-Volmer equation predicts an increase in the Tafel slope with temperature. This phenomenon, also observed for other systems, may be a consequence of factors such as the entropic contribution to the free energy of activation or changes in hydrogen coverage and has been tentatively discussed in the literature [9–11]. The insert in Fig. 4 shows the corresponding

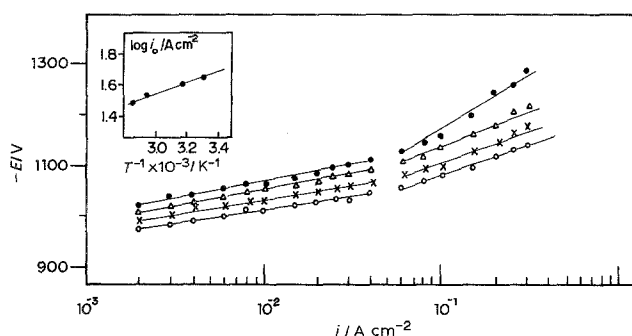


Fig. 4. Tafel plots for the HER on the electrode E3 in 28% KOH at different temperatures. Insert shows the Arrhenius plot for the HER. Key: (●) 25°C, (Δ) 40°C, (×) 60°C and (○) 80°C.

Table 4. Temperature dependence of the electrochemical parameters for the HER on the electrode E3 in 28% KOH

$T/^\circ\text{C}$	$b/mV\text{dec}^{-1}$	$-\eta_{135}/mV$	$-\eta_{250}/mV$	$i_0/A\text{cm}^{-2} \times 10^{-4}$
25	58	168	138	1.86
40	55	152	167	2.14
60	50	134	198	2.75
80	48	118	244	3.39

b : Tafel slope in the low c.d. region, i_0 : exchange current, η_{135} and η_{250} : overpotentials at c.d. 135mA cm^{-2} and 250mA cm^{-2} , respectively.

Arrhenius plot from which the energy of activation of the reaction was calculated as being 10.6kJ mol^{-1} . This value is similar to that obtained by Vandenborre *et al.* [5] for NiS_x electrodes.

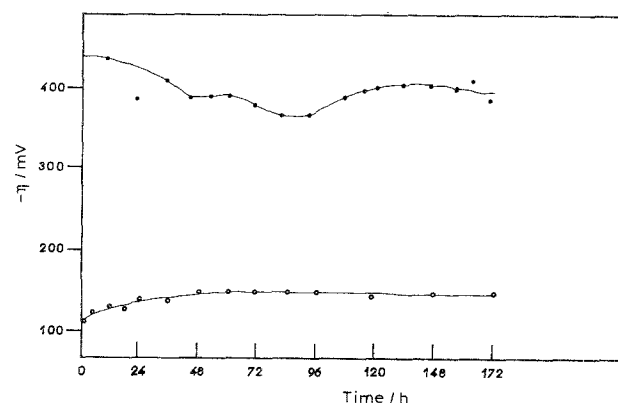
3.1. Mechanism of the HER

In order to obtain information on the mechanistic pathway of the HER on the E3 electrode, steady-state polarization curves were recorded at 25°C for different pHs. The results showed no dependence of the kinetics of the HER on pH.

The kinetic parameters obtained lead to the conclusion that the most probable mechanism in the low current density region under low coverage involves a first electron transfer (Volmer step) as a rate determining step followed by a fast electrochemical desorption (Heyrovsky step) [14].

3.2. Long term operation studies

With the purpose of evaluating the stability of the electrode E3 a continuous operation study was conducted at 70°C and 135mA cm^{-2} . The result of this experiment is presented in Fig. 5 and shows that the electrode potential increased somewhat during the first 50 h of polarization but then remained practically constant for up to 172 h. The data obtained from a long term experiment on a mild steel electrode are also plotted in order to establish a comparison with the conventional electrode material.

Fig. 5. Long term operation curve on electrode (○) E3 and (●) on mild steel in 28% KOH at 70°C. ($i = 135\text{mA cm}^{-2}$).

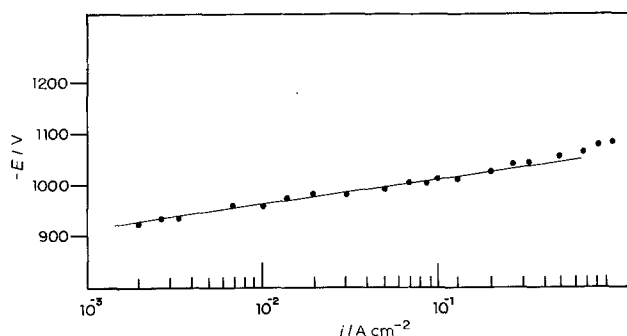


Fig. 6. Tafel plot for the HER on the electrode E3 in a chlor-alkali cell solution at 70°C.

3.3. Complementary studies

Figure 6 shows Tafel plot for the HER on the electrode E3 at 70°C in a solution similar to those employed in chlor-alkali cells (155 g dm⁻³ NaOH and 165 g dm⁻³ NaCl). At a current density (c.d.) of 210 mA cm⁻² the electrode potential is -1.070 V which is significantly lower than the value of -1.220 V observed for the conventional material (mild steel) under the same conditions. Although more detailed studies are needed the results show possible potential applications of this material in chlor-alkali cells.

Acknowledgements

Thanks are due to the Conselho Nacional de Desenvolvimento Científico e Tecnológico (CNPq) and to the Financiadora de Estudos e Projetos (FINEP), Brazil, for financial support.

References

- [1] E. R. Gonzalez, L. A. Avaca, A. C. Carubelli, A. A. Tanaka and G. Tremiliosi Filho, *Int. J. Hydrogen Energy* **9** (1984) 689.
- [2] J. de Carvalho, G. Tremiliosi Filho, L. A. Avaca and E. R. Gonzalez, *ibid.* **14** (1989) 61.
- [3] M. J. de Giz, S. A. S. Machado, L. A. Avaca and E. R. Gonzalez, Proceedings of the 175th Meeting of the Electrochemical Society, Los Angeles, 89 (1989) 1583.
- [4] A. C. D. Angelo, E. R. Gonzalez and L. A. Avaca, *Int. J. Hydrogen Energy* **16** (1991) 1.
- [5] H. Vandenborre, P. H. Vermeiren and R. Leysen, *Electrochim. Acta* **29** (3) (1984) 297.
- [6] K. Yamakawa, H. Tubakino, K. Akiyoshi, H. Inoue and K. Yoshimoto, Proceedings of the 172nd Meeting of the Electrochemical Society, Hawaii, 87 (1987) 2.
- [7] A. Nidola and R. Schira, *Int. J. Hydrogen Energy* **11** (1986) 449.
- [8] R. Sabela and I. Paseka, *J. Appl. Electrochem.* **20** (1990) 500.
- [9] B. E. Conway and L. Bai, *Int. J. Hydrogen Energy* **11** (1986) 583.
- [10] E. Gileadi, *J. Electrochem. Soc.* **134** (1987) 117.
- [11] B. E. Conway, D. F. Tessier and P. Wilkinson, *ibid.* **199** (1986) 249.
- [12] M. M. Jaksic, *J. Mol. Catalysis* **38** (1986) 161.
- [13] R. R. Chianelli, T. A. Pecoraro, T. R. Halbert, W. H. Pan and E. I. Stiefel, *J. Catal.* **86** (1984) 226.
- [14] L. P. Bicelli, *La Chim. e l'Industria* **55** (1973) 792.